

THE CANADIAN MINERALOGIST

Volume 50

June 2012

Part 3

The Canadian Mineralogist
Vol. 50, pp. 585-592 (2012)
DOI: 10.3749/canmin.50.3.585

THE CRYSTAL STRUCTURE OF SVYATOSLAVITE AND EVOLUTION OF COMPLEXITY DURING CRYSTALLIZATION OF A $\text{CaAl}_2\text{Si}_2\text{O}_8$ MELT: A STRUCTURAL AUTOMATA DESCRIPTION

SERGEY V. KRIVOVICHEV[§]

Department of Crystallography, St. Petersburg State University, University Emb. 7/9, 199034 St. Petersburg, Russia

ELENA P. SHCHERBAKOVA AND TURSUN P. NISHANBAEV

Institute of Mineralogy, Russian Academy of Sciences, 456317 Miass, Russia

ABSTRACT

The structure of svyatoslavite, a pseudo-orthorhombic polymorph of $\text{CaAl}_2\text{Si}_2\text{O}_8$, has been solved from a crystal twinned on (100) and refined to an R_1 value of 0.024, calculated for the 1788 unique observed ($|F_o| \geq 4\sigma_F$) reflections. The structure is monoclinic, $P12_11$, a 8.220(5), b 8.951(5), c 4.828(5) Å, β 90.00(5)°, V 355.2(5) Å³. The structure of svyatoslavite is based on a three-dimensional framework of SiO_4 and AlO_4 tetrahedra with Ca^{2+} ions at the interstitial sites. There are two Ca sites, $\text{Ca}1$ and $\text{Ca}2$, with occupancy factors of 0.919(4) and 0.081(4), respectively. The $\text{Ca}1$ site is coordinated by six O atoms with $\text{Ca}1\text{--O}$ bond lengths in the range 2.417–2.599 Å, with one long seventh $\text{Ca}1\text{--O}$ bond of 3.068 Å. The $\text{Ca}2$ site is 6-coordinated with $\text{Ca}2\text{--O}$ bond lengths in the range 2.380–2.775 Å. Framework of tetrahedra in svyatoslavite, as well as tetrahedral frameworks in other $\text{M}^{2+}[\text{Al}_2\text{Si}_2\text{O}_8]$ polymorphs ($\text{M}^{2+} = \text{Ba}^{2+}, \text{Ca}^{2+}$), is based on an orthogonal network, *i.e.*, a network with the angles between adjacent edges equal to either 90 or 180°. Growth of orthogonal nets is modeled using structural automata, which are finite automata adapted for the description of crystal structures. State diagrams for svyatoslavite and dmisteinbergite automata consist of four states each. The anorthite automaton is more complex as it contains eight states. The paracelsian automaton is remarkable in that it consists of 16 states and its state diagram has the topology of a four-dimensional cube (hypercube). During crystallization of the $\text{Ca}[\text{Al}_2\text{Si}_2\text{O}_8]$ melt, metastable phases with the svyatoslavite and dmisteinbergite topologies form first and then either dissolve or transform to anorthite. In terms of complexity of structural automata, this means that the less complex phases (svyatoslavite and dmisteinbergite) evolve into more complex anorthite structures. The observed sequence of phases corresponds to the increasing structural complexity of the solid system.

Keywords: svyatoslavite, dmisteinbergite, anorthite, structural complexity, finite automata, minerals of coal dumps; topological information content.

[§] E-mail address: skrivovi@mail.ru

INTRODUCTION

Svyatoslavite is a monoclinic (pseudo-orthorhombic) polymorph of $\text{CaAl}_2\text{Si}_2\text{O}_8$, first described as a mineral species by Chesnokov *et al.* (1989) from coal dumps of mine #45 near the city of Kopeysk, Chelyabinsk area, southern Urals, Russia. The mineralogy of the coal dumps of the Chelyabinsk coal area has recently been described in detail by Chesnokov *et al.* (2008). Svyatoslavite, along with anorthite and dmisteinbergite (a hexagonal or pseudo-hexagonal polymorph of $\text{CaAl}_2\text{Si}_2\text{O}_8$, Chesnokov *et al.* 1990), formed in the area of 'black blocks', which are products of extensive combustion of clays and carbonate rocks under reducing conditions at temperatures normally in the range 500–900 °C, but, in some cases, up to 1200 °C. The 'black blocks' are rich in carbon (graphite, coal) that forms as a result of reduction of methane. Svyatoslavite, anorthite and dmisteinbergite were found as crystals on the surface of coal and burned wood.

Svyatoslavite and dmisteinbergite are known to be metastable polymorphs of $\text{CaAl}_2\text{Si}_2\text{O}_8$, which crystallize in the $\text{CaO-Al}_2\text{O}_3\text{-SiO}_2$ system prior to crystallization of anorthite. They were first identified by Davis & Tuttle (1952), and their degree of stability, nucleation, and growth kinetics were investigated in detail by Abe *et al.* (1991), Daniel *et al.* (1995), and Abe & Sunagawa (1995). Abe *et al.* (1991) reported that pseudo-hexagonal (dmisteinbergite) and pseudo-orthorhombic (svyatoslavite) polymorphs nucleate prior to anorthite and grow in a supercooled $\text{CaAl}_2\text{Si}_2\text{O}_8$ melt until anorthite starts to crystallize. At that moment, these phases either dissolve or transform to anorthite. Daniel *et al.* (1995) described another metastable polymorph of $\text{CaAl}_2\text{Si}_2\text{O}_8$ with an unknown framework structure.

Takéuchi & Donnay (1959) determined the space groups of synthetic dmisteinbergite and svyatoslavite as hexagonal $P6/mmm$ and orthorhombic $P2_12_12_1$, respectively. They also determined the structure of the hexagonal polymorph and showed that it is based on double sheets of 6-membered rings of AlO_4 and SiO_4 tetrahedra (see also Dimitrijevic *et al.* 1999). Takéuchi *et al.* (1973) reported the structure of synthetic svyatoslavite to be monoclinic, $P12_11$ with $\beta = 90^\circ$, which results in pronounced twinning on the (100) plane. Recently, Hwang *et al.* (2010) reported the discovery of kumdykulite, an orthorhombic polymorph of albite, $\text{NaAlSi}_3\text{O}_8$. They proposed possible space-groups $P2nn$ and $Pmnn$, $a = 8.24$, $b = 8.68$, $c = 4.84$ Å, but it is probable that, by analogy to the synthetic pseudo-orthorhombic $\text{CaAl}_2\text{Si}_2\text{O}_8$ polymorph, kumdykulite also is monoclinic with probable pseudo-merohedral twinning on the (100) plane. Ito (1976) found that metastable hexagonal $\text{CaAl}_2\text{Si}_2\text{O}_8$ has monoclinic symmetry and forms twinned crystals, but did not report a structure determination.

In this paper, we report results of the crystal-structure refinement of svyatoslavite, compare it with data

from synthetic material, and discuss the topological relations between aluminosilicate frameworks in known $\text{M}^{2+}\text{Al}_2\text{Si}_2\text{O}_8$ polymorphs ($\text{M} = \text{Ca}, \text{Ba}$) using the theory of structural automata (Shevchenko *et al.* 2010). This theory coupled with orthogonal representation of complex nets (Krivovichev 2011) allows a quantitative evaluation of algorithmic topological complexity and provides a tool for comparison of the complexity of different types of frameworks.

EXPERIMENTAL

A crystal of svyatoslavite was mounted on a STOE IPDS II X-ray diffractometer equipped with an image plate area detector and operated at 50 kV and 40 mA. More than a hemisphere of three-dimensional data was collected using monochromatic $\text{MoK}\alpha$ X-radiation, with frame widths of 2° in w , and with a 2 min count for each frame. The unit-cell parameters (Table 1) were refined using least-squares techniques. The intensity data were integrated and corrected for Lorentz, polarization, and background effects using the STOE X-Red program. An analytical absorption correction was made on the basis of the experimentally determined crystal shape.

The SHELX programs (Sheldrick 2008) were used for determination and refinement of the crystal structure. The structure was solved in the monoclinic space-group $P12_11$ by direct methods and refined to an R_1 value of 0.024, calculated for the 1788 unique observed ($|F_o| \geq 4\sigma_F$) reflections. During the refinement, a pseudo-merohedral twinning model was applied using the $[-1\ 0\ 0\ /\ 0\ 1\ 0\ /\ 0\ 0\ 1]$ matrix. Final atom coordinates and

TABLE 1. CRYSTALLOGRAPHIC DATA AND REFINEMENT PARAMETERS FOR SVYATOSLAVITE

a (Å)	8.220(5)
b (Å)	8.951(5)
c (Å)	4.828(5)
β (°)	90.00(5)
V (Å ³)	355.2(5)
Space group	$P12_11$
F_{000}	276
Z	4
Crystal size (mm)	0.12 0.14 0.22
Radiation	$\text{MoK}\alpha$
Total Ref.	3214
Unique Ref.	1789
Unique $ F_o \geq 4\sigma_F$	1788
R_{int}	0.036
R_1	0.024
wR_2	0.064
S	1.086

Note: $R_1 = \sum ||F_o| - |F_c|| / \sum |F_o|$; $wR_2 = \{ \sum [w(F_o^2 - F_c^2)^2] / \sum [w(F_o^2)^2] \}^{1/2}$; $w = 1 / [\sigma^2(F_o^2) + (aP)^2 + bP]$, where $P = (F_o^2 + 2F_c^2) / 3$; $S = \{ \sum [w(F_o^2 - F_c^2)] / (n - p) \}^{1/2}$ where n is the number of reflections and p is the number of refined parameters.

TABLE 2. COORDINATES, DISPLACEMENT PARAMETERS (\AA^2), AND SITE-OCCUPANCY FACTORS (S.O.F.) OF ATOMS IN THE STRUCTURE OF SVYATOSLAVITE

Atom	s.o.f.	x	y	z	U_{eq}	
Ca1	0.919(4)	0.74926(10)	0.47314(9)	0.8554(2)	0.0118(2)	
Ca2	0.081(4)	0.7526(17)	0.4962(11)	0.662(2)	0.024(3)	
Al1	1	0.07023(13)	0.34176(16)	0.3974(2)	0.0079(3)	
Al2	1	0.56514(13)	0.13918(15)	0.8973(3)	0.0069(3)	
Si1	1	0.95079(14)	0.15317(13)	0.9024(2)	0.0074(3)	
Si2	1	0.44897(13)	0.32920(14)	0.3900(2)	0.0063(3)	
O1	1	0.0658(3)	0.1826(4)	0.1703(7)	0.0089(6)	
O2	1	0.0295(4)	-0.0019(3)	0.7630(6)	0.0106(7)	
O3	1	0.7656(3)	0.1396(3)	-0.0006(5)	0.0165(6)	
O4	1	0.9572(3)	0.3018(4)	0.6939(6)	0.0106(6)	
O5	1	0.5605(3)	0.2936(4)	0.6601(7)	0.0095(6)	
O6	1	0.5369(4)	0.4718(4)	0.2226(6)	0.0117(6)	
O7	1	0.2698(3)	0.3763(3)	0.4783(6)	0.0159(6)	
O8	1	0.4441(4)	0.1773(4)	0.1883(7)	0.0116(6)	

Atom	U_{11}	U_{22}	U_{33}	U_{23}	U_{13}	U_{12}
Ca1	0.0071(2)	0.0096(3)	0.0186(4)	-0.0024(2)	-0.0008(5)	0.0000(3)
Ca2	0.0079(5)	0.0084(8)	0.0074(6)	0.0003(5)	-0.0003(4)	0.0008(5)
Al1	0.0056(5)	0.0075(7)	0.0075(7)	-0.0002(4)	0.0008(4)	-0.0006(5)
Al2	0.0065(4)	0.0083(7)	0.0076(6)	0.0002(4)	-0.0002(4)	0.0004(4)
Si1	0.0045(4)	0.0075(6)	0.0070(5)	-0.0010(4)	-0.0005(4)	-0.0001(4)
Si2	0.0062(11)	0.0113(13)	0.0091(13)	-0.0015(12)	-0.0036(12)	0.0016(10)
O1	0.0066(14)	0.0091(15)	0.0162(14)	-0.0017(12)	-0.0039(9)	-0.0007(9)
O2	0.0034(10)	0.0321(15)	0.0139(11)	0.0054(10)	0.0016(10)	0.0005(11)
O3	0.0095(10)	0.0113(14)	0.0111(14)	0.0007(11)	0.0013(12)	0.0010(11)
O4	0.0118(11)	0.0091(14)	0.0075(12)	0.0022(12)	-0.0017(12)	-0.0018(10)
O5	0.0147(14)	0.0094(13)	0.0108(13)	0.0028(11)	-0.0030(9)	-0.0002(12)
O6	0.0073(12)	0.0256(14)	0.0146(12)	-0.0097(10)	-0.0006(10)	0.0035(11)
O7	0.0151(12)	0.0084(12)	0.0112(14)	-0.0029(11)	-0.0002(13)	-0.0033(11)
O8	0.0071(2)	0.0096(3)	0.0186(4)	-0.0024(2)	-0.0008(5)	0.0000(3)

TABLE 3. SELECTED BOND-LENGTHS (\AA) IN THE STRUCTURE OF SVYATOSLAVITE

Ca1-O1	2.417(3)	Ca2-O1	2.380(12)
Ca1-O5	2.425(3)	Ca2-O8	2.400(13)
Ca1-O4	2.425(3)	Ca2-O5	2.405(13)
Ca1-O8	2.431(4)	Ca2-O4	2.425(13)
Ca1-O6	2.488(4)	Ca2-O2	2.726(14)
Ca1-O2	2.599(3)	Ca2-O6	2.775(13)
Ca1-O3	3.068(4)	<Ca2-O>	2.512
<Ca1-O>	2.550		
Al1-O7	1.714(3)	Al2-O3	1.720(3)
Al1-O4	1.744(3)	Al2-O8	1.755(4)
Al1-O2	1.797(3)	Al2-O5	1.796(4)
Al1-O1	1.798(4)	Al2-O6	1.812(4)
<Al1-O>	1.763	<Al2-O>	1.771
Si1-O3	1.597(3)	Si2-O7	1.590(3)
Si1-O1	1.624(3)	Si2-O5	1.626(3)
Si1-O4	1.669(4)	Si2-O8	1.673(4)
Si1-O2	1.672(3)	Si2-O6	1.675(3)
<Si1-O>	1.641	<Si2-O>	1.641

displacement parameters of the atoms are given in Table 2, selected interatomic distances are in Table 3. A listing of structure factors and a cif file are available from the Depository of Unpublished Data on the Mineralogical Association of Canada website [Svyatoslavite CM50_585].

RESULTS

The structure of svyatoslavite is based on a three-dimensional framework of SiO_4 and AlO_4 tetrahedra with Ca^{2+} ions at the interstitial sites (Fig. 1a). There are two *Ca* sites, *Ca1* and *Ca2*, with occupancy factors of 0.919(4) and 0.081(4), respectively. The *Ca1* site is coordinated by six O atoms with the *Ca1*-O bond lengths in the range 2.417-2.599 \AA , with one long seventh *Ca1*-O bond equal to 3.068 \AA . The *Ca2* site is 6-coordinated with the *Ca2*-O bond lengths in the range 2.380-2.775 \AA . The symmetry of the $[\text{Al}_2\text{Si}_2\text{O}_8]^{2-}$ framework corresponds to the space group $P12_1/n1$; the *Ca1* and *Ca2* sites are related by the *n* glide-plane. However, owing to the dramatically different occupan-

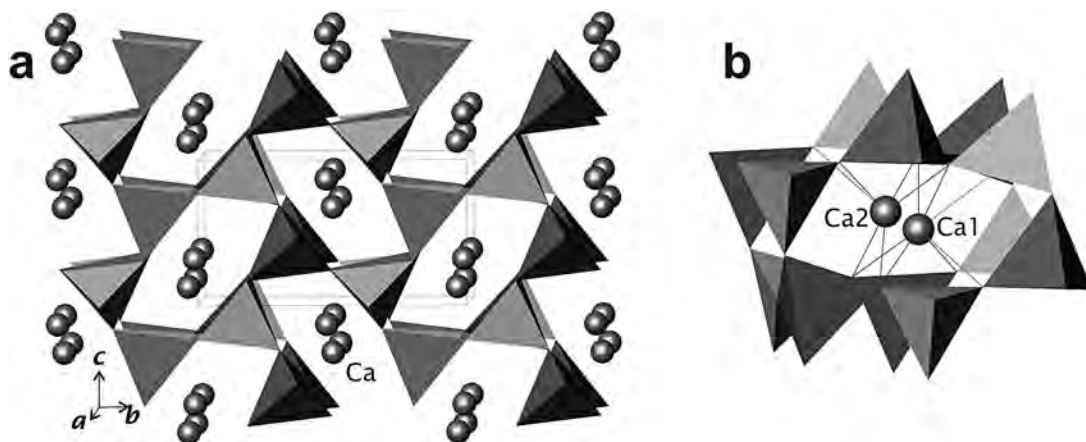


FIG. 1. Crystal structure of svyatoslavite viewed approximately along the *a* axis (a) and coordination of Ca^{2+} cations in the framework cavity (b).

cies of the *Ca1* and *Ca2* sites, the symmetry of the structure is reduced from $P12_1/n1$ to $P12_1$. It is of interest that, in synthetic svyatoslavite, the occupancies of the *Ca* sites are 0.403(4) and 0.564(5), respectively, *i.e.*, the distribution of Ca over the two sites in the synthetic material is more disordered than in the mineral. This difference between the synthetic and natural svyatoslavite structures results in significantly different *b* unit-cell parameters: 8.621 Å for the synthetic and 8.951 Å for the mineral. The *a* and *c* unit-cell parameters are almost equal: 8.228 and 4.827 Å for the synthetic and 8.220 and 4.828 Å for the mineral.

To explain the observed difference in the *b* unit-cell parameter, one has to analyze the positions of the Ca sites in the framework cavities. Figure 2a shows a nodal representation of the framework of tetrahedra in svyatoslavite (black and white nodes correspond to the Al and Si sites, respectively). The network underlying the svyatoslavite tetrahedron framework consists of four-membered rings that link together, creating six- and eight-membered rings. The Ca sites are located inside channels outlined by eight-membered rings and extending along the *c* axis. In the synthetic sample, where the distribution of Ca in the channels is more disordered, the eight-membered rings are shorter along the *b* axis, in comparison with the mineral with the more ordered arrangement of Ca. Figure 2b shows the geometrical parameters of the eight-membered ring in terms of the Al–Si distances around and across the ring. Whereas the Al–Si distances along the *a* axis are very similar, the Al–Si distances along the *b* axis in the mineral are longer, which leads to the elongation of its *b*-repeat distance in comparison to that of the synthetic crystal.

DISCUSSION

The framework of tetrahedra in svyatoslavite can be compared to the frameworks in other $\text{M}^{2+}[\text{Al}_2\text{Si}_2\text{O}_8]$ polymorphs ($\text{M}^{2+} = \text{Ba}^{2+}, \text{Ca}^{2+}$). Figure 3 shows networks that serve as underlying topologies in dmisteinbergite, anorthite, and paracelsian. The dmisteinbergite network is two-dimensional, whereas all others are three-dimensional. All four networks consist of four-membered rings linked in different fashions, resulting in distinct topologies. The important observation is that the networks shown in Figures 2a and 3 can be topologically (*i.e.*, without breaking any bonds) transformed into networks with the angles between adjacent edges being equal to 90 or 180° (adjacent edges are defined as having exactly one vertex in common). The resulting networks are shown in Figure 4. They can also be considered as obtained from a regular **pcu** net (Delgado Friedrichs *et al.* 2003) by removal of some of its edges. Krivovichev (2011) defined such networks as being orthogonal and showed that orthogonal nets are the most important ones for framework structures in zeolites, metal-organic structures, polymorphs of silica, etc. The growth of orthogonal nets can be modeled using structural automata proposed by Shevchenko *et al.* (2010) for modeling self-assembly processes for lovozerite-type structures [similar ideas have been used by Krivovichev (2004, 2010) to apply cellular automata to investigate the origin of structural diversity in complex inorganic structures]. In order to describe the automata, generating networks shown in Figure 4, we first consider some general definitions of finite automata and their application to crystal structures.

A deterministic finite automaton (DFA), *A*, is defined (Hopcroft *et al.* 2001) as

$$A = \{K, \Sigma, \delta, k_0, F\},$$

where $K = \{1, 2, 3, 4, \dots\}$ is the finite set of states, Σ is the finite set of transitional symbols (*e.g.*, **a**, **b**, **c**, etc.), δ is a transition function, k_0 is an initial state, **F** is a set of accepting states from K . The transition-function arguments are relevant to the current state and the transitional symbol; the result is a new state. For instance, the expression $\delta(k_1, \mathbf{a}) = k_2$ implies that, under the current state k_1 and the symbol **a**, the new state of the DFA will be k_2 .

For the description of crystal structures, we shall use the construction of DFA suggested by Morey *et al.* (2002), which we define as a structural automaton (Shevchenko *et al.* 2010). According to this construction, a state corresponds to a net vertex with a certain configuration of adjacent edges. Symbols of the set Σ are vectors (directed edges). The transition function identifies a transition from state k_1 to state k_2 via a vector **v** that belongs to the set Σ : $\delta(k_1, \mathbf{v}) = k_2$. For each vector (symbol) **v**, there exists a vector **v** such as $\delta(k_2, \mathbf{v}) = k_1$ (both **v** and **v** belong to the set Σ). One can also say that structural automata are bidirectional. Any state from K may be initial (k_0) and any state from K is accepting.

To generate an orthogonal network, one needs six vectors (symbols) defined in Figure 5a: $\Sigma = \{\mathbf{a}, \underline{\mathbf{a}}, \mathbf{b}, \underline{\mathbf{b}}, \mathbf{c}, \underline{\mathbf{c}}\}$. A simple infinite one-dimensional network is shown in Figure 5b. It consists of two different alternating vertex configurations, **1** and **2**. A transition from vertex **1** to vertex **2** occurs via vectors **a** and **b**, whereas,

because of the property of bidirectionality, transition from **2** to **1** occurs via vectors **a** and **b**. The diagram of transition from one state to another is depicted in Figure 5c. However, as structural automata are always bidirectional, this diagram can be shortened to the diagram shown in Figure 5d. This diagram is called a state diagram of the structural automaton. From a mathematical point of view, it represents a directed labeled graph. The complexity of this graph defines a complexity of the corresponding structural automaton.

Figure 6 shows state diagrams for finite structural automata generating the nets shown in Figure 4. The svyatoslavite and dmisteinbergite automata consist of four states each; however, the topology of the state diagrams is different, which results in topologically distinct networks. The state diagram for the dmisteinbergite automaton has the topology of a quadrilateral, whereas the svyatoslavite state diagram has the topology of a tetrahedron. In contrast, the automaton for anorthite is more complex, as it contains eight states; its state diagram has the topology of a square antiprism. The paracelsian automaton (Fig. 6d) is remarkable in that it consists of 16 states, and its state diagram has a topology of a 4-dimensional cube (hypercube).

The discussion of complexity of frameworks of tetrahedra provided above is based upon the concepts of structural automata and state diagrams. As related to nets, a state diagram for the automaton that generates the net is in fact identical to its quotient graph. A quotient graph is a compressed description of

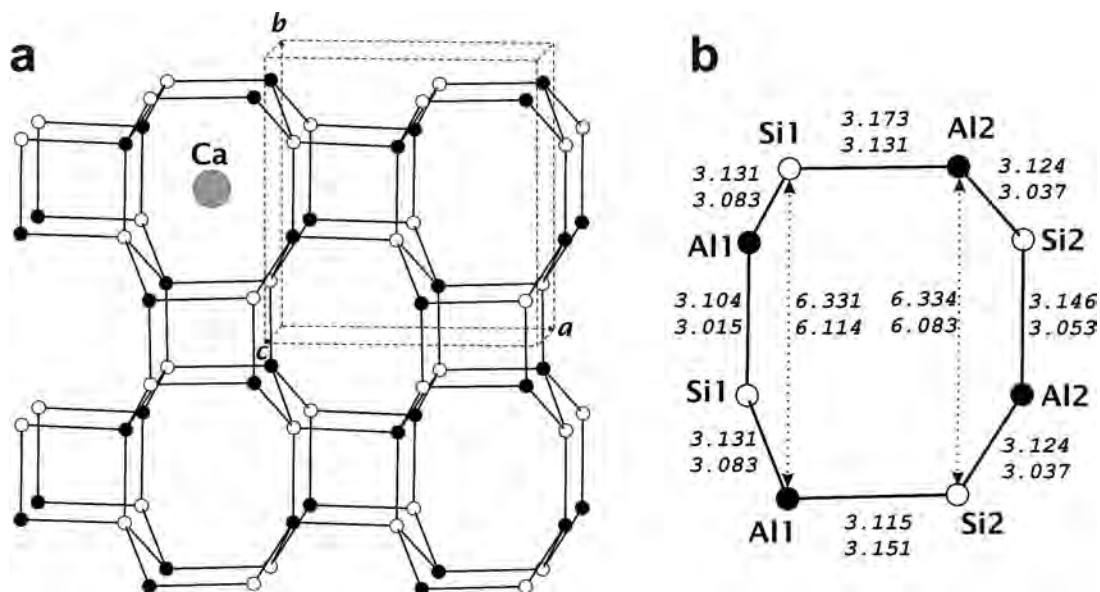


FIG. 2. Nodal representation of svyatoslavite framework of tetrahedra (a: black and white nodes symbolize AlO₄ and SiO₄ tetrahedra, respectively) and geometrical characteristics of svyatoslavite and synthetic svyatoslavite (b: upper and lower numbers correspond to natural and synthetic samples, respectively).

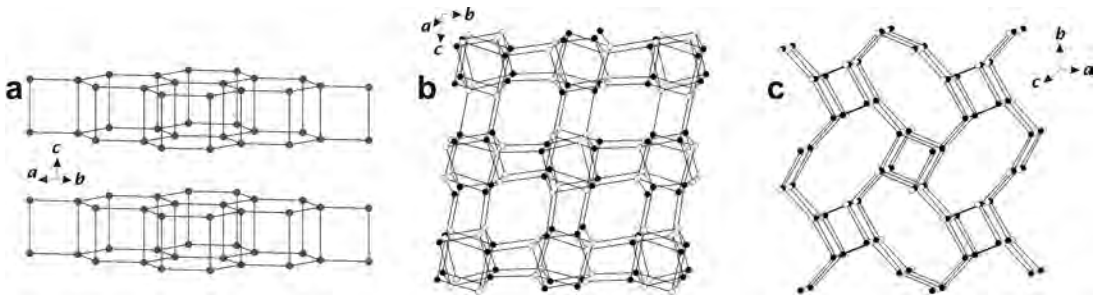


FIG. 3. Nodal representation of frameworks of tetrahedra in the $M^{2+}[Al_2Si_2O_8]$ polymorphs ($M^{2+} = Ba^{2+}, Ca^{2+}$): (a) dmisteinbergite, (b) anorthite, and (c) paracelsian.

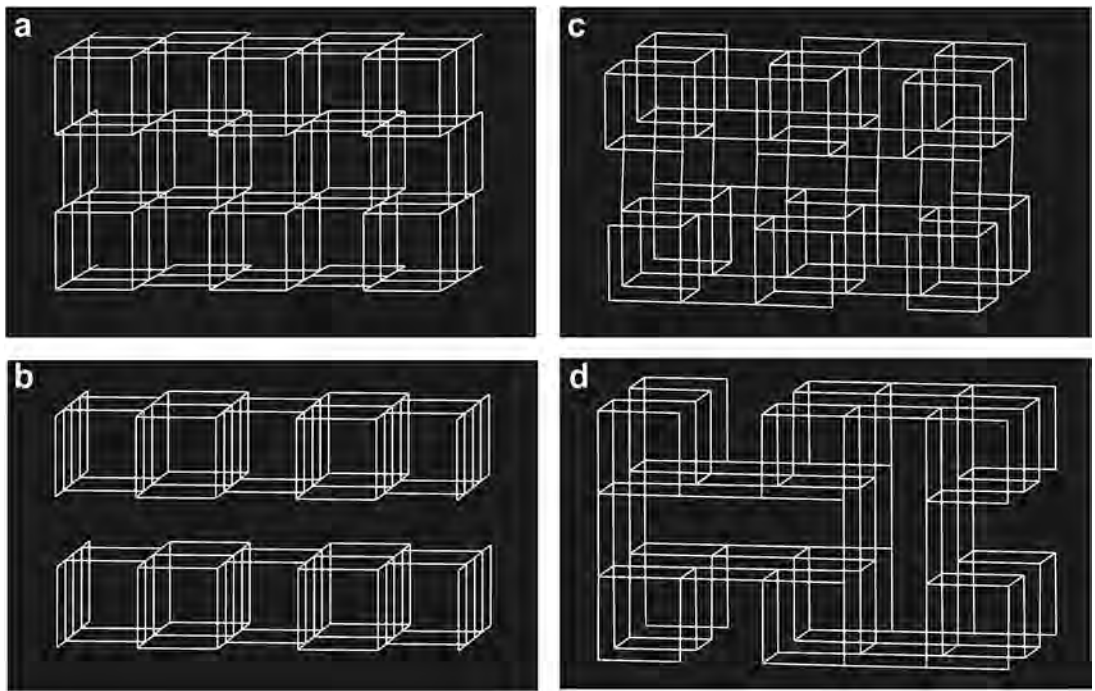


FIG. 4. Orthogonal representations of network topologies in (a) svyatoslavite, (b) dmisteinbergite, (c) anorthite, and (d) paracelsian.

topology of a periodic net and is widely used in modern mathematical crystallography (Klee 2004, Blatov & Proserpio, 2011). The difference between the common definition of a quotient graph and the one used in this paper is that, for orthogonal networks, the number of transitional symbols (= vectors that provide transitions between adjacent vertices) are expressed in terms of three orthogonal vectors, **a**, **b**, and **c**, and their reciprocal counterparts, **a**, **b**, and **c**.

As mentioned above, during crystallization of the $Ca[Al_2Si_2O_8]$ melt, the metastable phases with svyatoslavite and dmisteinbergite topologies form first, and then either dissolve or transform into anorthite. In terms of complexity of their structural automata, this means that the less complex phases (svyatoslavite and dmisteinbergite) evolve into the more complex anorthite structure. Thus, the observed sequence of phases corresponds to the increasing structural complexity of

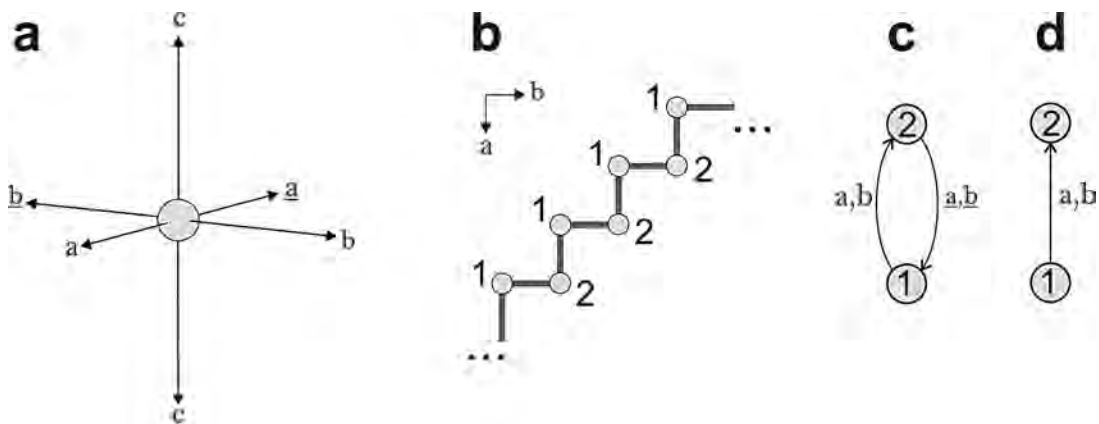


FIG. 5. (a) Orthogonal vector basis. (b) One-dimensional orthogonal network consisting of two states. (c) Extended and (d) shortened state diagrams of its structural automaton.

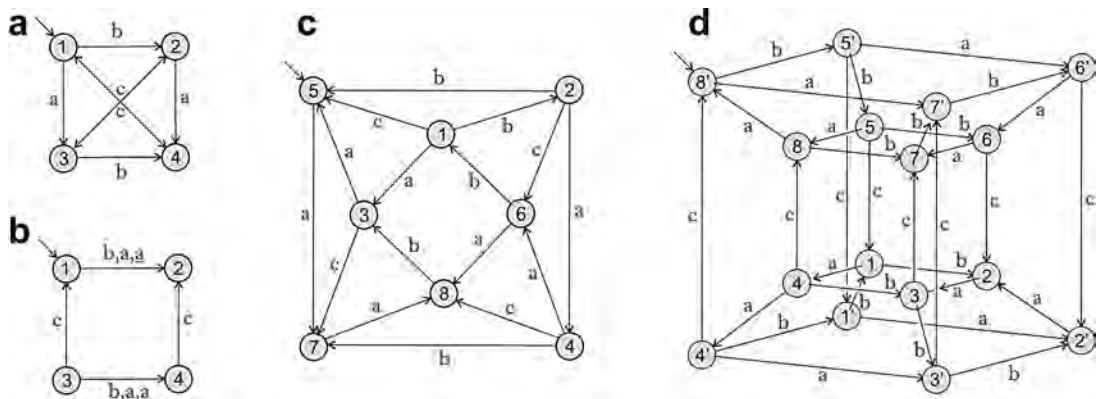


FIG. 6. State diagrams of structural automata generating network topologies in (a) svyatoslavite, (b) dmisteinbergite, (c) anorthite, and (d) paracelsian.

the system. This is in agreement with the principle of simplicity, which was defined Goldsmith (1953) as “...some measure of the complexity of the distribution of individual or particular atoms or atomic groups in a phase, irrespective of space group chemistry”. According to Goldsmith (1953), phases with higher simplicity (= lower complexity) crystallize more easily than phases with lower simplicity (= higher complexity). This principle is especially important for metastable phases that crystallize under non-equilibrium conditions, when the reaction rate is high. This is the case for the appearance of metastable svyatoslavite and dmisteinbergite phases during rapid crystallization of the $\text{Ca}[\text{Al}_2\text{Si}_2\text{O}_8]$ melt. This is obviously the case for the appearance of svyatoslavite and dmisteinbergite during combustion reactions in coal dumps as well, when

these minerals occur in a gaseous transfer environment, similar to a field of fumarole activity. Their metastable appearance in nature is thus can be ascribed to their lower complexity compared to anorthite.

The approach to evaluation of structural complexity developed in this paper is based upon the algorithmic complexity of structural topologies expressed in terms of structural automata. Another approach was developed recently, which is based upon the use of Shannon information theory (Krivovichev 2012) and will be discussed elsewhere.

ACKNOWLEDGEMENTS

We are grateful to Frank C. Hawthorne and Robert F. Martin for the useful comments and polishing the

English, which improved the manuscript considerably. This work was supported through the Russian Federation Grant-in-Aid Programme 'Cadres' (contract # 16.740.11.0490 to S.V.K.).

REFERENCES

- ABE, T. & SUNAGAWA, I. (1995) Hexagonal $\text{CaAl}_2\text{Si}_2\text{O}_8$ in a high temperature solution; metastable crystallization and transformation to anorthite. *Mineralogical Journal* **17**, 257-281.
- ABE, T., TSUKAMOTO, K., & SUNAGAWA, I. (1991) Nucleation, growth and stability of $\text{CaAl}_2\text{Si}_2\text{O}_8$ polymorphs. *Physics and Chemistry of Minerals* **17**, 473-484.
- BLATOV, V.A. & PROSERPIO, D.M. (2011) Periodic-graph approaches in crystal-structure prediction. In *Modern Methods of Crystal Structure Prediction* (A.R. Oganov, ed.), Wiley-VCH Verlag GmbH & Co. KGaA, Weinheim, 1-28 p.
- CHESNOKOV, B.V., LOTOVA, E.V., PAVLYUCHENKO, V.S., NIGMATULINA, E.N., USOVA, L.V., BUSHMAKIN, A.F., & NISHANBAEV, T.P. (1989) Svyatoslavite $\text{CaAl}_2\text{Si}_2\text{O}_8$ (orthorhombic) - a new mineral. *Zapiski Vsesoyuznogo Mineralogicheskogo Obshchestva* **118**(2), 111-114 (in Russian).
- CHESNOKOV, B.V., LOTOVA, E.V., NIGMATULINA, E.N., PAVLYUCHENKO, V.S., & BUSHMAKIN, A.F. (1990) Dmishteinbergite $\text{CaAl}_2\text{Si}_2\text{O}_8$ (hexagonal) - a new mineral. *Zapiski Vsesoyuznogo Mineralogicheskogo Obshchestva* **119**(3), 43-46 (in Russian).
- CHESNOKOV, B.V., SHCHERBAKOVA, E.P., & NISHANBAEV, T.P. (2008) *Minerals from Burned Dumps of Chelyabinsk Coal Basin*. Miass, Institute of Mineralogy UrO RAS, 139 p. (in Russian).
- DANIEL, I., GILLET, P., MCMILLAN, P.F., & RICHEL, P. (1995) An in-situ high-temperature structural study of stable and metastable $\text{CaAl}_2\text{Si}_2\text{O}_8$ polymorphs. *Mineralogical Magazine* **59**, 25-33.
- DAVIS, G.L. & TUTTLE, O.F. (1952) Two new crystalline phases of the anorthite composition, $\text{CaO} \cdot \text{Al}_2\text{O}_3 \cdot 2\text{SiO}_2$. *American Journal of Science*, Bowen Volume, 107-114.
- DELGADO FRIEDRICH O., O'KEEFFE, M., & YAGHI, O.M. (2003) Three-periodic nets and tilings: regular and quasi-regular nets. *Acta Crystallographica* **A59**, 22-27.
- DIMITRIJEVIC, R., DONDUR, V., & KREMENOVIC, A. (1999) Thermally induced phase transformations of Ca-exchanged LTA and FAU zeolite frameworks: Rietveld refinement of the hexagonal $\text{CaAl}_2\text{Si}_2\text{O}_8$ diphylosilicate structure. *Zeolites* **16**, 294-300.
- GOLDSMITH, J.R. (1953) A "simplicity principle" and its relation to "ease" of crystallization. *Journal of Geology* **61**, 439-451.
- HOPCROFT, J.E., MOTWANI, R., & ULLMAN, J.D. (2001) *Introduction to Automata Theory, Languages and Computation*. Addison-Wesley, Boston.
- HWANG, S.-L., SHEN, P., CHU, H.-T., YUI, T.-F., LIU, J.G., & SOBOLEV, N.V. (2010) Kumdykolite, an orthorhombic polymorph of albite, from Kokchetav ultrahigh-pressure massif, Kazakhstan. *European Journal of Mineralogy* **21**, 1325-1334.
- ITO, J. (1976) High temperature solvent growth of anorthite on the join $\text{CaAl}_2\text{Si}_2\text{O}_8$ - SiO_2 . *Contributions to Mineralogy and Petrology* **59**, 187-194.
- KLEE, W.E. (2004) Crystallographic nets and their quotient graphs. *Crystal Research and Technology* **39**, 959-968.
- KRIVOVICHEV, S.V. (2004) Crystal structures and cellular automata. *Acta Crystallographica* **A60**, 257-262.
- KRIVOVICHEV, S.V. (2010) Actinyl compounds with hexavalent elements (S, Cr, Se, Mo) - structural diversity, nanoscale chemistry, and cellular automata modeling. *European Journal of Inorganic Chemistry* **2010**, 2594-2603.
- KRIVOVICHEV, S.V. (2011). Topological variations in inorganic oxocompounds: origin of structural diversity. *Acta Crystallographica* **A67**, C15.
- KRIVOVICHEV, S.V. (2012) Topological complexity of crystal structures: quantitative approach. *Acta Crystallographica* **A68**, 393-398.
- MOREY, J., SEDIG, K., MERCER, R.E., & WILSON W. (2002) Crystal lattice automata. In *CIAA 2001, LNCS 2494* (B.W. Watson & D. Wood, eds.). Springer-Verlag, Berlin-Heidelberg, pp. 214-220.
- SHELDRIK, G.M. (2008) A short history of *SHELX*. *Acta Crystallographica* **A64**, 112-122.
- SHEVCHENKO, V.YA., KRIVOVICHEV, S.V., & MACKAY, A.L. (2010) Cellular automata and local order in the structural chemistry of the lovozerite-group minerals. *Glass Physics and Chemistry* **36**, 1-9.
- TAKÉUCHI, Y. & DONNAY, G. (1959) The crystal structure of hexagonal $\text{CaAl}_2\text{Si}_2\text{O}_8$. *Acta Crystallographica* **12**, 465-470.
- TAKÉUCHI, Y., HAGA, N., & ITO J. (1973) The crystal structure of monoclinic $\text{CaAl}_2\text{Si}_2\text{O}_8$: a case of monoclinic structure closely simulating orthorhombic symmetry. *Zeitschrift für Kristallographie* **137**, 380-398.

Received October 22, 2011, revised manuscript accepted June 13, 2012.